

**Realization of a Single-Chip, SiGe:C-Based Power Amplifier
for Multi-Band WiMAX Applications**

Journal:	<i>IET Microwaves, Antennas & Propagation</i>
Manuscript ID:	Draft
Manuscript Type:	Research Paper
Date Submitted by the Author:	
Complete List of Authors:	Kaynak, Mehmet; Sabanci University, FENS Tekin, Ibrahim; Sabanci University, FENS Gurbuz, Y; Sabanci University, Electronics Engineering
Keyword:	POWER AMPLIFIERS, INTEGRATED CIRCUIT DESIGN, SILICON-GERMANIUM



Realization of a Single-Chip, SiGe:C-Based Power Amplifier for Multi-Band WiMAX Applications

Mehmet Kaynak, Ibrahim Tekin and Yasar Gurbuz

*Sabanci University, Faculty of Engineering and Natural Sciences, Tuzla, 34956, Istanbul, Turkey
Tel: +90(216) 483 9533, e-mail: yasar@sabanciuniv.edu*

Abstract—A fully-integrated Multi-Band PA using 0.25 μm SiGe:C process with an output power of above 25 dBm is presented. The behaviour of the amplifier has been optimized for multi-band operation covering, 2.4 GHz, 3.6 GHz and 5.4 GHz (UWB-WiMAX) frequency bands for higher 1-dB compression point and efficiency. Multi-band operation is achieved using multi-stage topology. Parasitic components of active devices are also used as matching components, in turn decreasing the number of matching component. Measurement results of the PA provided the following performance parameters: 1-dB compression point of 20.5 dBm, gain value of 23 dB and efficiency value of %7 operation for the 2.4 GHz band; 1-dB compression point of 25.5 dBm, gain value of 31.5 dB and efficiency value of %17.5 for the 3.6 GHz band; 1-dB compression point of 22.4 dBm, gain value of 24.4 dB and efficiency value of %9.5 for the 5.4 GHz band. Measurement results show that using multi-stage topologies and implementing each parasitic as part of the matching network component has provided a wider-band operation with higher output power levels, above 25 dBm, with SiGe:C process.

Keywords— Power Amplifier, SiGe:C, Multi-Band, WiMAX, UWB, WLAN

I. INTRODUCTION

Worldwide interoperability for microwave access (WiMAX) is a new wireless technology that enables convergence of mobile and fixed broadband networks up to 70 km in line-of-sight (LOS) environments. IEEE 802.16-2004 standard is the first released of WiMAX operates at two different frequency ranges; 10-66 GHz frequency range for LOS environments and 2-11 GHz frequency range for non-LOS environments. IEEE 802.16-2004 standard is proposed for fixed deployments. IEEE 802.16e is intended primarily for both stationary and mobile deployments. IEEE 802.16e is planned for the three frequency bands namely, 2.5-2.9 GHz, 3.4-3.6 GHz and 5.2-5.9 GHz [1]. This standard is based on a multi-carrier modulation as the OFDM scheme (Orthogonal Frequency Division Multiplexing). WiMAX can be configured to use nominal bandwidth ranging between 1.25 MHz and 20 MHz. In WiMAX only 200 of 256 carriers are actually used. 192 of these are used for Data and 8 are used for Pilots. WiMAX has significantly more subcarriers than WLAN and more data in each symbol but it does not have a significantly higher data rate than WLAN. This is because, while making the carriers more closely, the symbol period must be increased, proportionally, to maintain the orthogonality of the individual carriers. The advantage of using longer symbol period is making the

channel more resistant to channel impairments such as multipath. So, major advantage of WiMAX is, it can operate over longer distances and in non-LOS applications.

Power Amplifiers (PAs) are key components in the wireless communications industry, consuming a great amount of power in overall transceiver. The PAs must achieve high operation efficiency in order to maximize the battery life and minimize the size and cost. The integration of analog and digital blocks on the same chip is becoming increasingly important in all transceivers. However, one of the drawbacks of WiMAX transceivers is its sensitivity to nonlinear distortions due to its greatly variable envelope and high peak to mean envelope power ratio values [2]. The nonlinearity is mostly generated from the power amplifier and results to expand the transmission spectrum into adjacent channels. Most practical way to achieve linear amplification is using Class-A power amplifiers with a high back-off, which corresponds to move the operating point of the amplifier into the linear region. However the efficiency of the amplifier degrades significantly due to the back-off which is very important aspect for the mobile communication. Using Class-AB or Class-B amplifier results a nonlinear amplifications, making it harder to operate such communications standards. In order to achieve both power efficiency and spectrum efficient standards such as WiMAX, several linearization techniques have been proposed in the literature and can be easily applied to highly-linear Class-A PAs [2]. These linearization methods allow designers to use Class-A power amplifiers without any back-off which keep the power efficiency levels within acceptable ranges.

From the technology perspective, for the past several years AlGaAs/GaAs heterojunction bipolar transistor (HBT) technologies are currently the preferred bipolar technologies for the commercial development of linear power amplifier (PA) modules for wireless handsets due to their excellent linearity and power-added efficiency (PAE) [3]. However, these types of integrated circuits are relatively expensive and significant efforts are being exerted to displace these HBT technologies with alternative bipolar technologies, such as Silicon (Si) bipolar junction transistor (BJT), or Silicon Germanium (SiGe) HBT [4]. The developments on SiGe technology was improved with carbon doping and carbon-doped SiGe:C process allow us to use transistors with 200 GHz of f_t values [5]. PA design is not only limited by the f_t values of the transistor but also BV_{CE0} (collector-emitter breakdown voltage), crucial for generating higher power. High-power transistor of used technology has BV_{CE0} values of 7 Volts, allowing designers to achieve higher voltage levels at the collector terminal of the transistor [5]. Provided the advantages of such technology, allowing a better optimization between f_t and BV_{CE0} , integrated solutions for transceivers, especially in the frequency range of 1 to 10 GHz frequency bands, more feasible with a better performance parameters, fulfilling the gap between Silicon and III-V group – based technologies.

In this work, a three stage fully integrated power amplifier was designed and fabricated using IHPs (Innovations for High Performance) SGB25VD technology. PA is optimized for multi-band operation covering WiMAX frequency bands, 2.5-2.9 GHz, 3.4-3.6 GHz and 5.2-5.9. Multi-Band operation

achieved using 3 stages by distributing the total gain to different stages for different frequency bands, as detailed in Section II. Transistor sizes and parasitic components were optimized to contribute to the output matching network, also contributing to the wide-band operation. In Section III, PA is analyzed for three WiMAX frequencies and measurement results shows that output powers above 25 dBm is achieved using HBT transistor with SiGe:C technology from fully integrated (including on-chip matching networks) power amplifier. For handling high current densities and high power in 2 mm² area, special layout techniques were also employed, as detailed in Section III.

II. DESIGN OF MULTI-STAGE PA

Figure 1 shows the schematic of the three-stage power amplifier. The design of the PA started with selecting the appropriate transistor in the technology library. IHPs SiGe:C high voltage transistor has f_{\max} of 70 GHz, β of 190 and collector-emitter breakdown voltage of 7 Volt, suitable for high-power, high-frequency circuit designs [5]. The transistor gives the maximum β while driven with 50-150 μ A base currents, also providing enough f_T values for the operation in the frequency band of interest.

DC operating points of the transistors also specify the parasitic components and also change the input and the output impedance of the transistor. The sizes of the transistors were adjusted to achieve the desired power level controlled with DC current level. For high output power levels, a higher-level DC current is required. This has been one of the major challenges of RFIC technologies due to the limitation on the provided metal-thickness by the technology.

A three stage topology which is shown in Fig. 1; first stage was used as a driving stage while also performing an impedance matching with the source. The use of a driver stage in high-power amplifier applications is preferred because of the transistors not giving the maximum output power and maximum gain at the same output impedance [6]. The second stage is also used as a gain stage while the third stage was for power delivery, handling large amount of power.

Modified current mirror type of bias circuit is used to bias the transistors as presented in Figure 2. It keeps the quiescent current constant, independent of temperature, by employing two diode connected transistors in series from the base of Q2 to the ground. R4 is N times R3, and the area of the power transistor in the connected stage is N times larger than the area of Q2 for a mirror ratio of N. Base biasing resistor is chosen approximately 10-15 times larger than 50 Ω to block the RF signal leakage that may cause a drop of output power and efficiency. By changing V_{ref} control voltage, one can set the quiescent current precisely during test and measurement.

To achieve a higher output power levels, larger sized transistors are necessary. However, larger-sized transistors decrease the input impedance of the transistor and bring difficulties for the input impedance matching to 50 Ω source. Also, increasing the maximum output power level may require a decrease in the gain of the amplifier. This can be explained by different required impedance values for load-pull simulations, specifying the maximum output power and gain-circles for the maximum gain conditions.

Furthermore, multi-stage PAs includes a last stage with higher output power level and high-gain driver stage. In this design, three-stage PA topology, as presented in Fig. 1, is used for achieving high-output power and high gain, simultaneously for the requirements of Multi-band WiMAX applications.

Load-Pull simulations are very important for finding the adequate impedance values, providing the maximum output power. Since the PA is designed for multi frequency bands, load pull simulations have been repeated for each band as presented in Figure 3. These simulations also specify the required output matching network component values. The maximum output powers can be achieved with low impedance values, as expected as shown in Figure 3. The last stage of the amplifier has a transistor total area of $64 \mu\text{m}^2$ and for load pull simulations this value is used. Due to the difference RF performance of transistor at different frequencies and different parasitics of transistors, required impedance values are changed but not particularly.

Output matching circuit is achieved by series capacitor and shunt inductor as presented in Figure 1. Inter-stage matching circuits are accomplished by only using series capacitors (C_{cp} 's). Input stage matching is also first order, output matching circuit, and it is achieved by shunt inductor and series capacitor.

Designs of matching circuits are rather complex since the characteristics of the matching networks change with the dc biasing, number of the parallel transistors in each stage, and the frequency. The impedance seen from the output of the last stage was optimized for a maximum output power, according to the load pull analysis, for achieving high compression points in each frequency band. Numbers of parallel transistors are 4, 8, and 16 for 1st, 2nd, and 3rd stage, respectively. The parallel connection of transistors protects the PA from thermal runaways, if the layout is drawn, carefully. Layout techniques used in this design are detailed in Section III.

III. MEASUREMENT RESULTS

Design and simulation of the power amplifier is performed using Cadence® SpectreRF simulator and Agilent Design System (ADS)® environments, supported by IHP technology library. Carefully designed circuit was fabricated using IHP's SGB25VD technology. Die photo of the fabricated PA is shown Figure 4, occupying an area of approximately $1 \times 2 \text{ mm}^2$. For increasing the current handling capability of metal paths in IC technologies, stacked metal layers are used. RC extraction is performed using Assura® tool under Cadence® environment. All the inductors are re-modeled with stacked metal layers. Also, long paths are extracted as an inductor for increasing the accuracy of the post-layout simulations. Inductive extraction is performed using Agilent ADS® MOMENTUM tool. Bypass capacitors (C_{cp} 's) are selected large enough to suppress the ground bounce and noise. Guard rings, which are typically a square ring of substrate contacts or well trenches, surrounding the active and passive devices, are also used in this work for improving the noise interference of the circuit. Transistor paralleling is the other main consideration of layout drawing. However, with many transistor, the base

drive to the outside transistors can be phased delayed compared to the shortest path. So, it is important to keep the line-lengths equal. Collector and emitter paths, which the DC and AC currents are handled, are drawn with wide and stacked metal. There is a common trade-off between the parasitic capacitance due to interconnection of parallel transistors and distance between the transistors. If the interval between the parallel transistors is small, thermal problems could occur due to the high power. Typically, 5 times of emitter-width distance is applied between parallel transistors. Parasitic capacitances generated from interconnection lines are a main consideration for transistor bandwidth, especially between base and emitter. The base-emitter connection lines are drawn carefully to decrease the parasitic capacitance value below few tens of femto-Farads. Parasitic capacitances into output matching networks are typically extracted and taken into account during the schematic design. Other important concept for high power RFIC applications is the grounding. Grounding of the circuit should be perfect at all the points on integrated circuit and is very crucial if the ground plane of the PA is not large enough. The free spaces of the layout were filled with ground plane, preventing the small voltage drops. All the capacitors, used in the layout, are MIM capacitors.

Figure 5 show the measured P_{out} vs. P_{in} characteristics of the PA at 3.6 GHz. Measured PAE performance of the PA is also given in Figure 5. As illustrated in Figure 5, PA has a 1-dB compression point of 25.5 dBm and power added efficiency of % 17.5 at 3.6 GHz operating frequency. Figure 6 summarize the compression point and gain performance of the PA for interested frequency bands for simulated and measured values. Measurement results show that the compression point of the PA is degraded 1-dB from simulation results almost for whole frequency range as illustrated in Figure 6. Figure 6 also shows that the measured power gain curve of the amplifier is quite shifted especially for lower frequency band. The measured gain of the PA is 23 dB, 31.5 dB and 24.4 dB for 2.4 GHz, 3.6 GHz and 5.2 GHz, respectively. The differences between measured and simulated results for power gain and 1-dB compression point are attributed to the still uncompensated parasitics and also insufficient extraction of the path inductances of the output stage.

Figure 7 and Figure 8 show that the S_{11} and S_{22} of the PA are below -10 dB at the frequency of interest, adequate for the desired/wireless applications. The large difference between measured simulated values of S_{22} of the PA also attributed to insufficient extraction of path inductances of the output stage.

Two-tone test is also performed for the Multi-Band PA. Two signals with 312.5 KHz frequency spacing were applied to the input of the PA and 1st and 3rd harmonic power levels were measured. The measurements were performed for the power levels for which the amplifier operates in linear region. The third order intercept point (IP3) is extrapolated using this low-power measurement results. The extrapolated output referred third order intercept point is 36 dBm. This measured and extrapolated data are presented Figure 9.

Error Vector Magnitude (EVM) setup was used for measuring the EVM performance of Multi-Band PA, as shown in Figure 10. The WiMAX modulated signal was generated using Agilent ADS software. The generated signal is uploaded to Agilent E8267D VSG signal generator. Signal generation was performed with a carrier frequency using the VSG signal generator. The modulated signal was supplied to the PA input and the output of the signal was captured using spectrum analyzer. The modulated signal was demodulated using Agilent VSA 89601 software with a limited bandwidth of 10 MHz. Then, demodulated signal was analyzed with Agilent ADS software. The constellation points, spectrum view, time domain view and RCE (EVM) performance of the demodulated signal can be analyzed using the setup in Fig. 10. The modulated signal was 802.16-2004 which has a carrier frequency of 3.6 GHz, bandwidth of 7 MHz, and modulation type of 64 QAM OFDM signal.

The measurement results for EVM performance is shown in Fig. 11. There was an unexpected increase in low power levels, coming from inadequate dynamic range of the measurement instruments. This could be seen on black line in Fig. 11. In order to eliminate this problem, a thru-line was also measured with same modulated signal for system calibration. The black curve is the EVM results of the whole system (PA + measurement setup) which also include the distortions from measurement setup. The blue curve was measured using on-chip thru-line, giving the distortion generated from the measurement setup for same power levels. The thick red line gives the EVM performance of the standalone PA. Typical acceptable EVM values for WiMAX protocol is below % 5-4, pointed using green line in Fig. 11. The suitable output power levels are up to 17 dBm output power, meaning that the PA is suitable using with a back-off of 8-10 db without a need for linearization. By adopting an appropriate linearization method, this back-off value could be decreased, further improving the efficiency of the amplifier [7].

The ACPR measurements were also performed for our PA. The signal bandwidth was taken as 3.25 MHz and spacing of the carriers was chosen 3.5 MHz. The result of ACPR measurements is given in Figure 12. As expected, the ACPR performance is degraded with increase of power levels.

Table 1 shows a comparison between our work and similar other works that were presented using comparable technologies with the one used here. Various performance parameters were achieved with different technologies and topologies such as lower output powers but higher efficiencies [8-10]; higher output powers/efficiencies using external matching networks [11-12]. When compared to other similar work, as in Table 1, our study presents the best optimum performance parameters in terms of 1-dB compression points, Gains, Efficiency and EVMs. Further advantage of our study, with respect to others, is that our PA is working in multiple frequency band/standards, meeting the performance requirements of all three bands, 2.4, 3.6 and 5.4 GHz). The better performance of our PA is due to the application of very careful design procedure, parasitic extraction and compensation, making good use of parasitics, such as in part of matching circuits and good utilization of technology and its advantages.

IV. CONCLUSION

A fully-integrated Multi-Band PA has been presented using 0.25 μm SiGe:C process with an output power of above 25 dBm. The behavior of the amplifier has been optimized for wide operating frequency range covering, 2.4 GHz, 3.6 GHz and 5.4 GHz (WiMAX) frequency bands for high 1-dB compression point and efficiency. Multi-Band operation has been achieved using multi-stage topology. Parasitic components of active devices were utilized, instead of compensation, in the matching circuits, greatly reducing the number of matching components and area. Measurement results of the PA provided the following performance parameters: 1-dB compression point of 20.5 dBm, gain value of 23 dB and efficiency value of %7 operation for the 2.4 GHz band; 1-dB compression point of 25.5 dBm, gain value of 31.5 dB and efficiency value of %17.5 for the 3.6 GHz band; 1-dB compression point of 22.4 dBm, gain value of 24.4 dB and efficiency value of %9.5 for the 5.4 GHz band. The results are better in many cases or comparable, when compared to the PAs using counterpart technologies and even III/V technology, as illustrated in Table 1. These results indicates that SiGe:C technology, or SiGe technology, can easily fill-in the gap even replace for certain (especially mid-power range) applications for the realization of single chip transceiver for wireless communication applications.

ACKNOWLEDGMENT

The authors would like to thank IHP for process and measurement support. This work was performed in the context of the network TARGET– “Top Amplifier Research Groups in a European Team” and supported by the Information Society Technologies Programme of the EU under contract IST-1-507893-NOE, <http://www.target-org.net/>.

REFERENCES

- [1] A. Amer, E. Hegazi and H. Ragai; “A Low-Power Wideband CMOS LNA for WiMAX” *IEEE Transactions on Circuits and Systems-II: Express Briefs*, vol. 54, pp. 4 – 8, Jan. 2007
- [2] G. Ducar, P. Mingo and J. Valdovinos; “Predistortion Method for Nonlinear Distortion Cancellation in WiMAX Transmitters” *Wireless Communication Systems*, 2006, pp. 786 - 790
- [3] K. Nellis and P.J. Zampardi; “Comparison of Linear Handset Power Amplifiers in Different Bipolar Technologies” *IEEE Journal of Solid-state Circuits*, vol. 39, pp. 1746-1754, Oct. 2004.
- [4] J. B. Johnson, A. J. Joseph, D.C. Sheridan, R. Maladi, P. Brandt, J. Persson, J. Andersson, A. Bjorneklett, U. Persson, F. Abasi, and L. Tilly “Silicon-Germanium BiCMOS HBT Technology for Wireless Power Amplifier Applications” *IEEE Journal of Solid-State Circuits*, vol. 39, pp. 1605-1614, Oct. 2004.
- [5] IHP 0.25 μm SiGe:C BiCMOS with High-Voltage Devices Process Parameters, <http://www.ihp-microelectronics.com/16.0.html>
- [6] S. C. Cripps, *Advanced Techniques in RF Power Amplifier Design*, Norwood: Artech House, INC, 2002.
- [7] M. Helaoui, S. Boumaiza, A. Ghazel and Fadhel M. Ghannouchi, “On the RF/DSP Design for Efficiency of OFDM Transmitters” *IEEE Transaction on Microwave Theory and Techniques*, vol. 53, no. 7, July 2005, pp. 2355-2361.
- [8] E. James Crescenzi, M. S. Wood, A. Prejs, S. Raymond and W. Pribble, “A 2.5 Watt 3.3-3.9 GHz Power Amplifier for WiMAX Applications using a GaN HEMT in a Small Surface-Mount Package” *Microwave Symposium, 2007. IEEE/MTT-S International*, 3-8 June 2007, pp: 1111-1114

- [9] Y. Ding and R. Harjani, "A high-efficiency CMOS 22 dBm linear power amplifier," *IEEE J. Solid-State Circuits*, vol. 40, no. 9, pp. 1895–1900, Sep. 2005.
- [10] A. Behzad et al., "Direct-conversion CMOS transceiver with automatic frequency control for 802.11a wireless LAN," *IEEE ISSCC Dig. Tech. Papers*, Feb. 2003, pp. 356–357.
- [11] M. Sagebiel, S. Gerlach, A. Kruck and V. Subramanian, "An EVM-optimized Power Amplifier for 2.4-GHz WLAN Application", *CSIC 2005 Digest*, pp 162-165, ISBN: 0-7803-9250-7/05
- [12] N. Tanzi, J. Dykstra and K. Hutchinson, "A 1-Watt Doubly Balanced Flip-Chip SiGe Power Amplifier" *IEEE Radio Frequency Integrated Circuits Symposium*, 2003
- [13] "SiGe Power amps Deliver +18dBm for 5 GHz WLANs" *EE times*, pp.28, Oct. 28, 2002

TABLE CAPTIONS

TABLE 1: A COMPARISON BETWEEN THIS DESIGN AND OTHER REFERENCES

FIGURE CAPTIONS

Figure 1: Three-Stage PA Schematic

Figure 2: Schematic of Bias Circuit

Figure 3: Load-Pull Simulation results

Figure 4: Die Photo of the fabricated PA

Figure 5: Measured P_{in} vs P_{out} and efficiency curve at 3.6 GHz

Figure 6: Measured vs. Simulated 1-dB Comp. and power gain

Figure 7: Measured vs. Simulated input matching performance

Figure 8: Measured vs. Simulated output matching performance

Figure 9: Measured OIP3

Figure 10: EVM Measurement Setup

Figure 11: Measured EVM (RCE)

Figure 12: Measured ACPR

Table 1

Technology	P_{1db}/P_{sat} (dBm)	Gain (dB)	% Efficiency (@1dB comp.)	EVM(%)/Back- Off (dB)	Reference
<i>0.25 SiGe:C</i>	<i>25.5/28</i>	<i>31.5</i>	<i>17.5</i>	<i>6.5/6</i>	<i>This work</i>
GaN	33/35	12.5	26	3/6	[8]
0.18 cmos	20.5/22	N/A	36	7.5/6	[9]
0.18 cmos	19/23	N/A	9	7.5/6.3	[10]
SiGe	27/-	33	42	4/6	[11]
0.35 SiGe	29/31.5	20.6	18.5	N/A	[12]
SiGe	18	22.8	N/A	N/A	[13]

Fig. 1

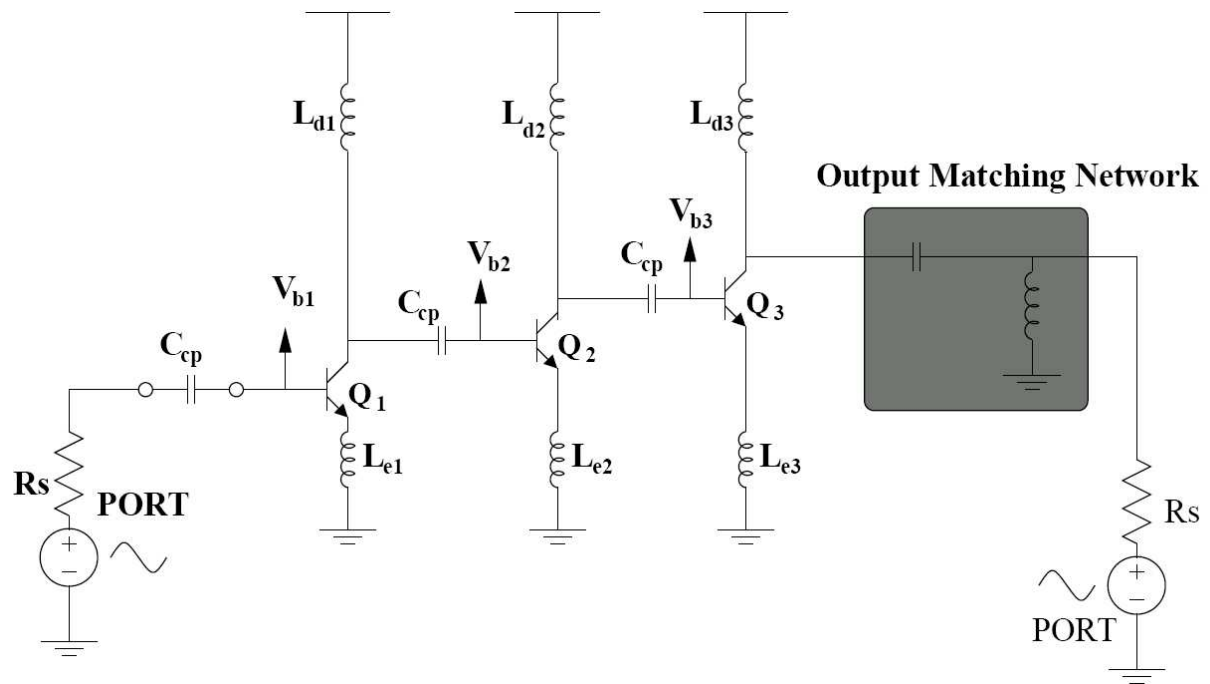


Fig. 2

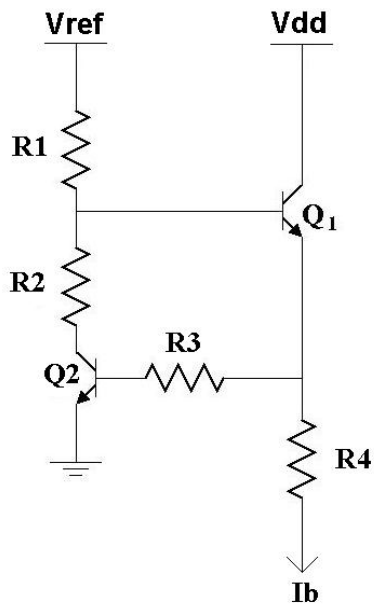


Fig. 3

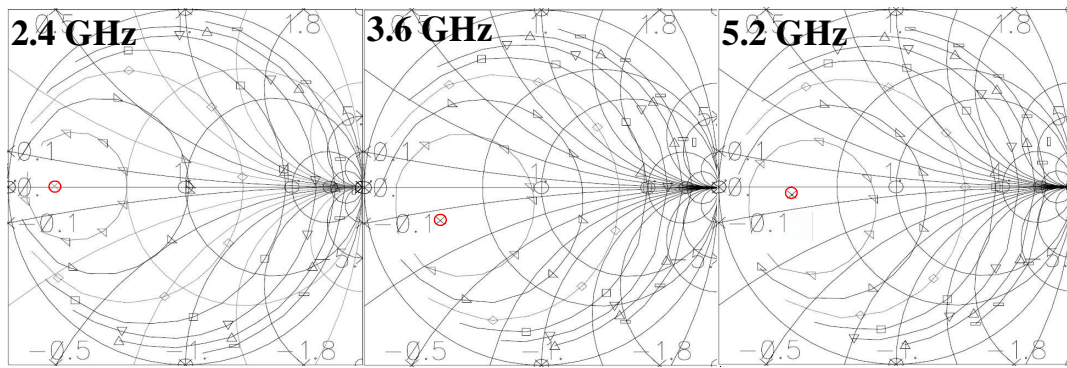


Fig. 4

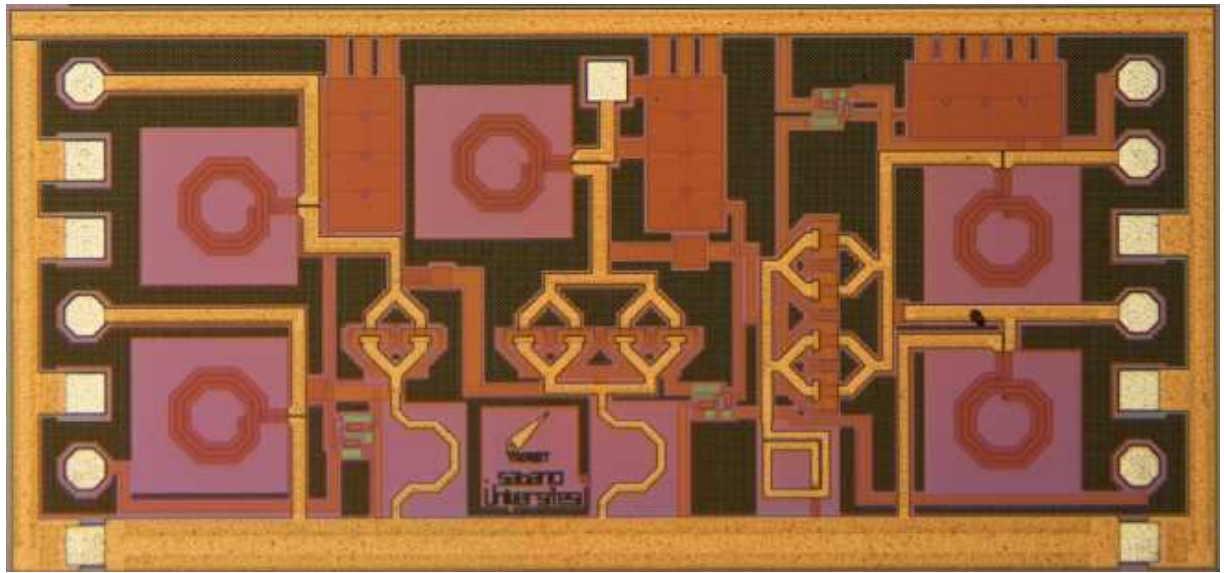


Fig. 5

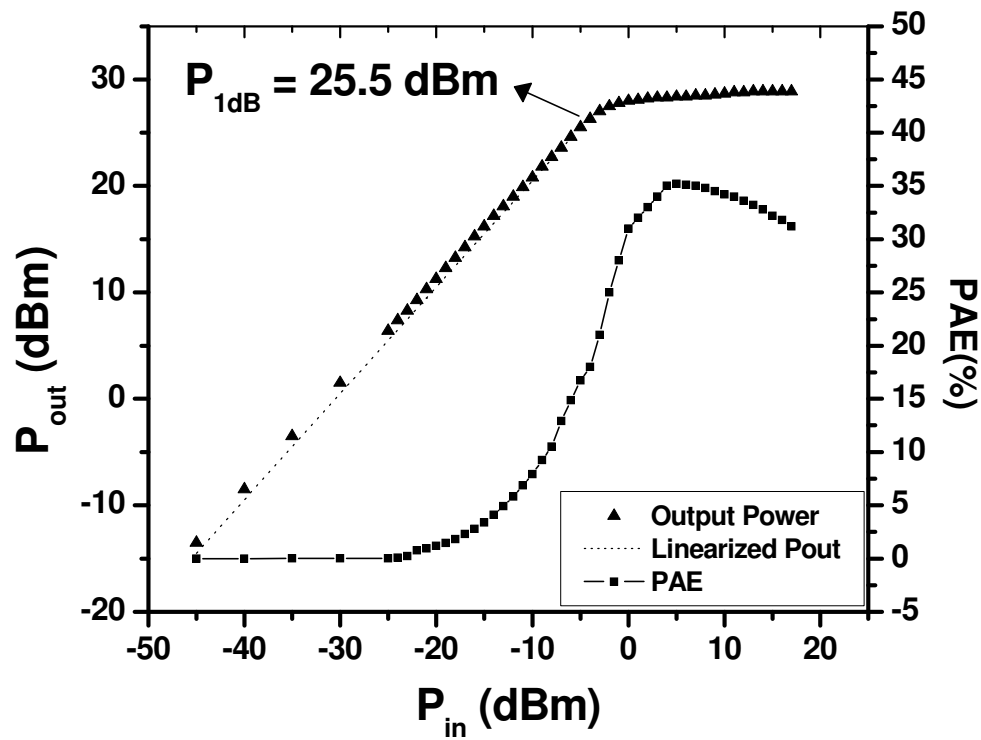


Fig. 6

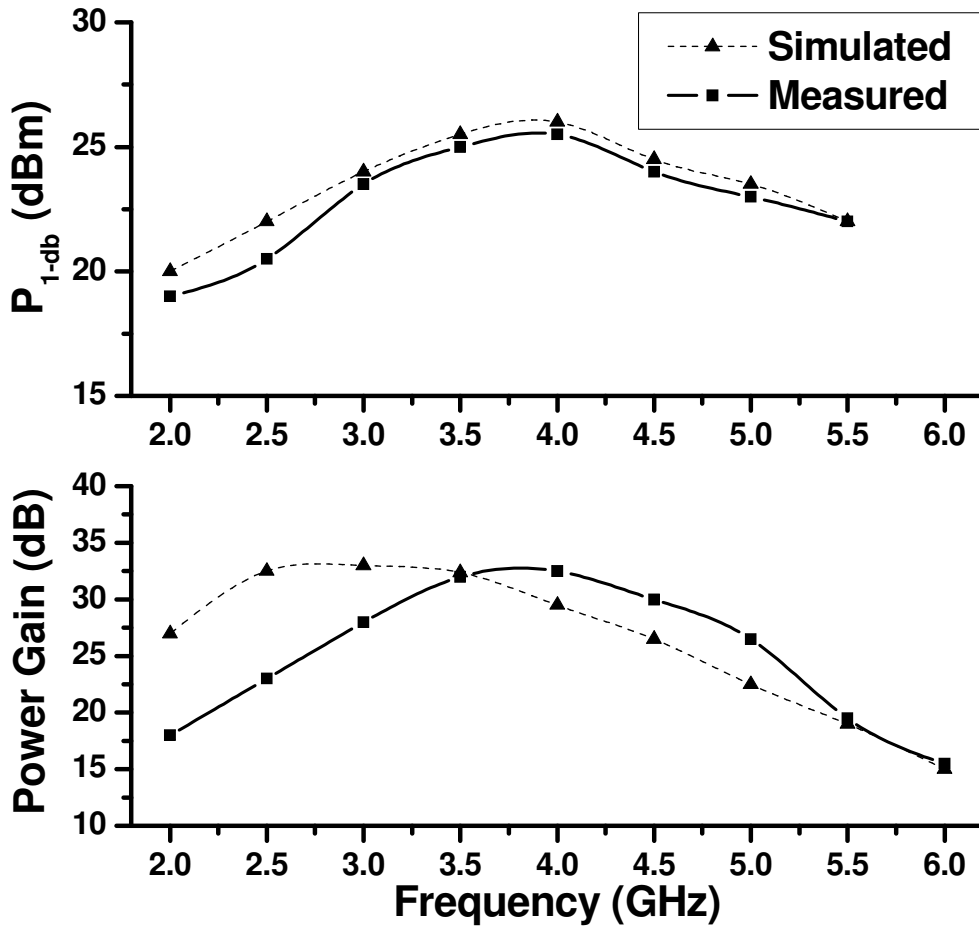


Fig. 7

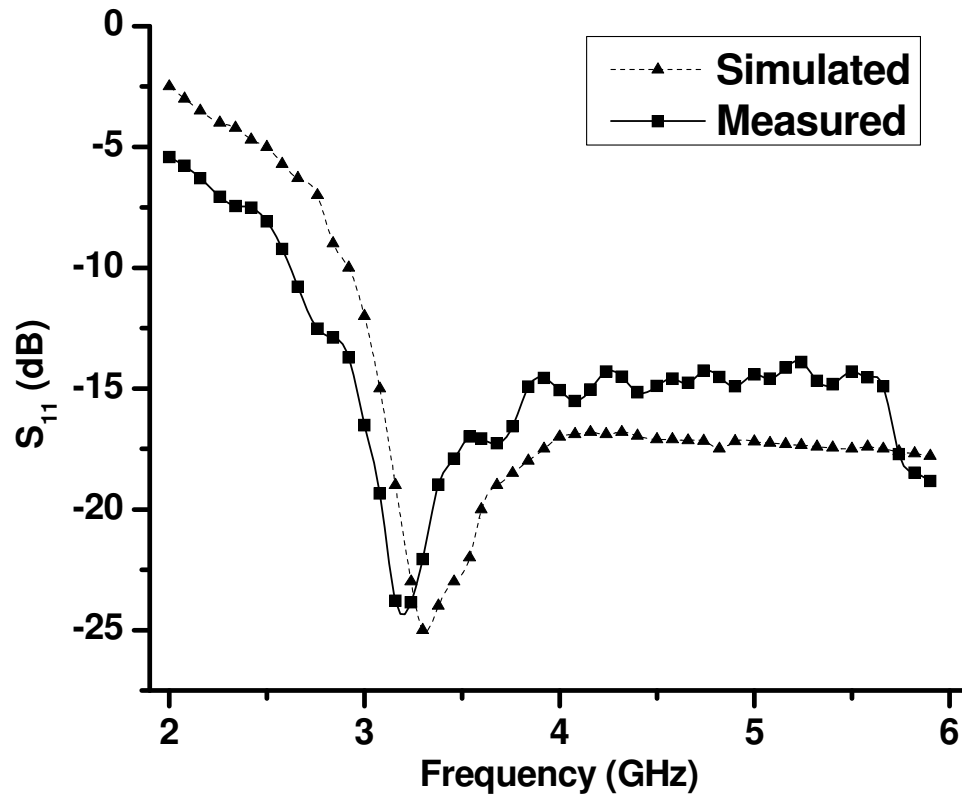


Fig. 8

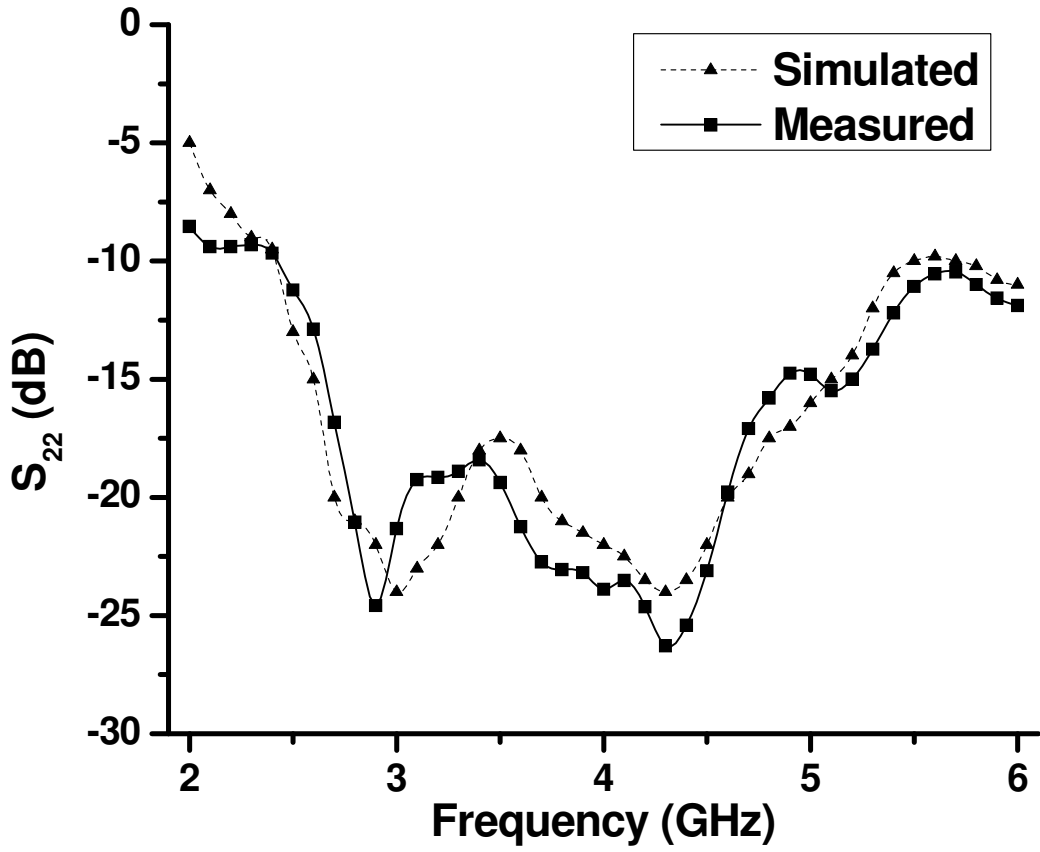


Fig. 9

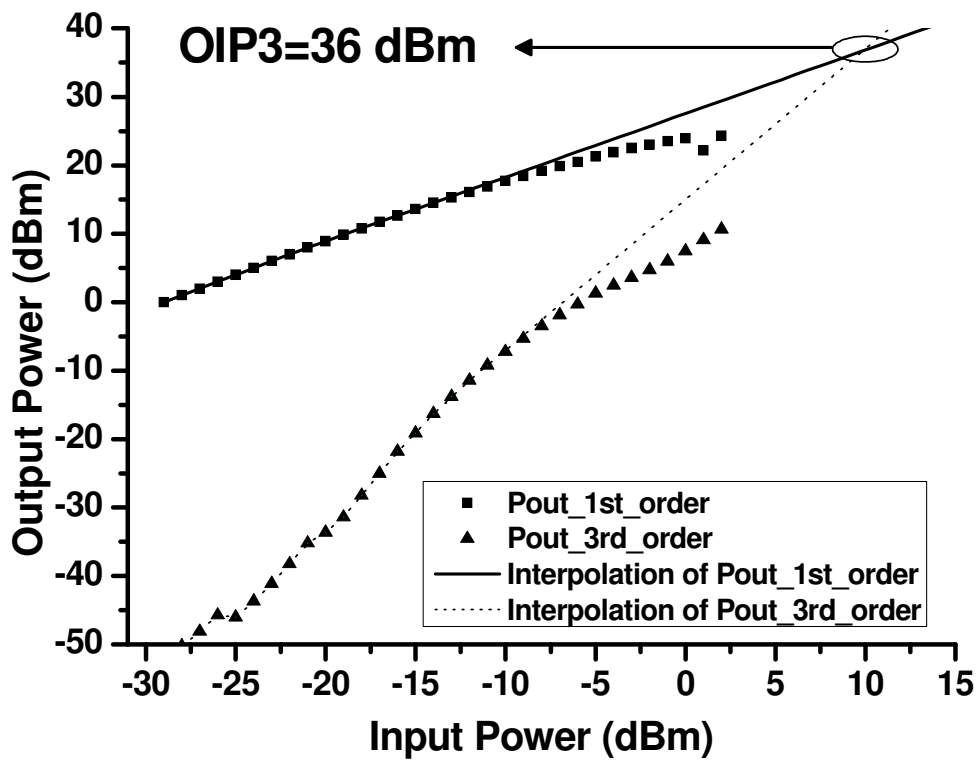


Fig. 10

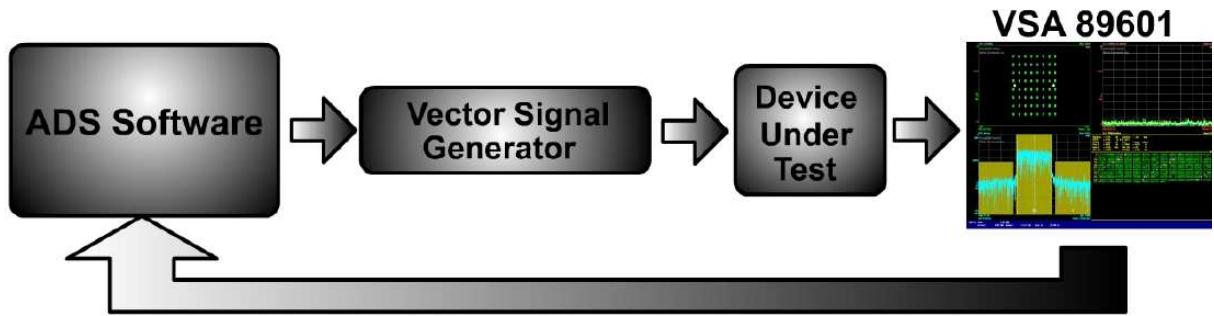


Fig. 11

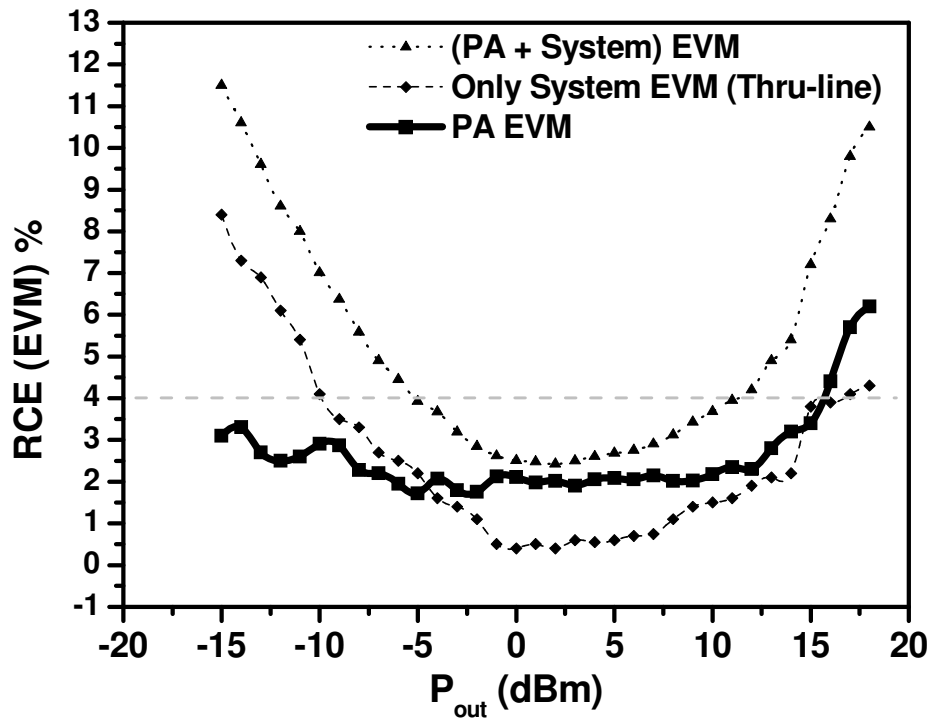


Fig. 12

